Available online at www.sciencedirect.com
ScienceDirect
Journal of Nuclear Materials 367–370 (2007) 930–934
journal of nuclear materials
www.elsevier.com/locate/jnucmat

The synergistic influence of temperature and displacement rate on microstructural evolution of ion-irradiated Fe–15Cr–16Ni model austenitic alloy

T. Okita [a], T. Sato [a], N. Sekimura [a], T. Iwai [b], F.A. Garner [c,*]

[a] Department of Quantum Engineering and Systems Science, University of Tokyo, Japan
[b] Research Center for Nuclear Science and Technology, University of Tokyo, Japan
[c] Pacific Northwest National Laboratory, Richland, WA 99352, USA

Abstract

An experimental investigation of microstructural evolution has been conducted on Fe–15Cr–16Ni irradiated with 4.0 MeV nickel ions. Irradiations proceeded to dose levels ranging from ~0.2 to ~17 dpa at temperatures of 300, 400, 500 and 600 °C at dpa rates of 1×10^{-4}, 4×10^{-4} and 1×10^{-3} dpa/s. The swelling was found to monotonically increase with decreases in dpa rate at every irradiation condition studied. The earliest and most sensitive component of microstructure to both temperature and especially dpa rate was found to be the Frank loops. The second most sensitive component was found to be the void microstructure, which co-evolves with the loop and dislocation microstructure.

1. Introduction

The experiment described in this paper is one of two companion experiments using identical specimens directed toward the study of the dependence of void swelling on dpa rate. The other experiment proceeded at seven different neutron-induced dpa rates between 8.9×10^{-9} and 1.7×10^{-6} dpa/s in FFTF-MOTA at ~430 °C [1,2]. In that experiment, the swelling of Fe–15Cr–16Ni was found to monotonically increase with decreases in dpa rate at every irradiation condition studied. The experiment described in this paper focused on the same model alloy using ion irradiation at four different temperatures and three different dpa rates between 1×10^{-4} and 1×10^{-3} dpa/s.

2. Experimental details

The model austenitic alloy, ternary Fe–15Cr–16Ni, was prepared by arc melting from very pure Fe, Ni and Cr. The alloy was rolled to sheets of 0.2 mm thickness. Afterward, standard 3 mm microscopy disks were then punched and annealed for 30 min at 1050 °C in a very high vacuum. The chemical composition of the alloy in wt% is Fe–15.01Cr–16.03Ni–0.012C–0.004Si–0.003Mn–0.01S and <0.0007Mo.

Irradiation proceeded with 4.0 MeV Ni^{3+} ions in the high fluence irradiation facility (HIT) operated

* Corresponding author. Tel.: +1 509 376 4136, mobile: +1 509 531 2112; fax: +1 509 376 0418.
E-mail address: frank.garner@pnl.gov (F.A. Garner).

0022-3115/$ - see front matter © 2007 Elsevier B.V. All rights reserved.
doi:10.1016/j.jnucmat.2007.03.061

by the University of Tokyo and located at Tokai-Mura, Japan. No gas atoms were preinjected or simultaneously injected. Two or three specimens were observed at every irradiation condition.

The four irradiation temperatures and three dpa rates chosen are listed in Table 1. Note that the trend with respect to dpa rate was established only at the lower two dose levels. For the highest dose level, 16–18 dpa, irradiation proceeded only at 4×10^{-4} dpa/s.

The damage vs. depth profile was calculated using the TRIM code [3] and is shown in Fig. 1. After irradiation the specimens were electrochemically thinned to reach a depth of 600–700 nm. This depth was chosen to avoid a strong influence of the 'injected interstitial' effect [4,5] and the implanted nickel and also to minimize the influence of the specimen surface. The uncertainty in depth was 10% at most, yielding a dpa and dpa rate uncertainty of ~10%, much smaller than the differences in the three dpa rates employed. Analysis of the loop microstructure by the dark field weak-beam method was conducted using a JEOL 200CX electron microscope operating at 200 KeV.

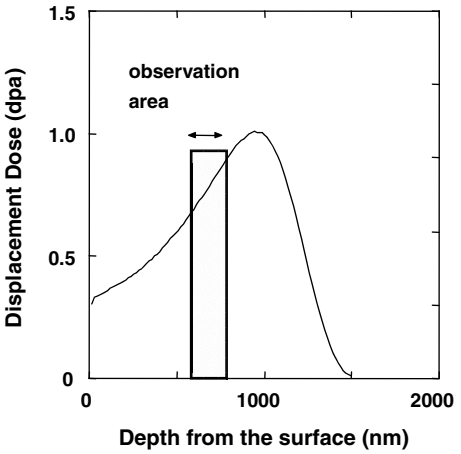

Fig. 1. Depth distribution of ion-induced damage as calculated by the TRIM code, showing a nominal 1.0 dpa maximum with the range of depths chosen for observation by microscopy.

Table 1
Irradiation conditions and microstructural data of Fe–15Cr–16Ni

Temperature (°C)	dpa[a]	dpa/s[a]	Dislocation loop density (m^{-3})	Void density (m^{-3})	Swelling (%)
300	0.17	1.0×10^{-4}	4.93×10^{22}	5.75×10^{21}	0.0060
		4.0×10^{-4}	4.51×10^{22}	5.40×10^{21}	0.0053
		1.0×10^{-3}	4.12×10^{22}	4.12×10^{21}	0.0045
	1.6	1.0×10^{-4}	9.89×10^{22}	5.19×10^{22}	0.038
		4.0×10^{-4}	8.32×10^{22}	4.52×10^{22}	0.032
		1.0×10^{-3}	7.40×10^{22}	4.42×10^{22}	0.020
	18.0	4.0×10^{-4}	1.01×10^{23}	5.23×10^{22}	0.042
400	0.18	1.0×10^{-4}	1.44×10^{22}	1.02×10^{21}	0.0071
		4.0×10^{-4}	1.10×10^{22}	8.90×10^{20}	0.0055
		1.0×10^{-3}	9.23×10^{21}	7.25×10^{20}	0.0048
	1.3	1.0×10^{-4}	6.10×10^{22}	5.92×10^{21}	0.054
		4.0×10^{-4}	5.20×10^{22}	5.76×10^{21}	0.037
		1.0×10^{-3}	2.18×10^{22}	4.55×10^{21}	0.022
	16.2	4.0×10^{-4}	8.90×10^{22}	9.90×10^{21}	0.054
500	0.17	1.0×10^{-4}	2.94×10^{21}	3.95×10^{21}	0.030
		4.0×10^{-4}	2.59×10^{21}	3.07×10^{21}	0.019
		1.0×10^{-3}	2.06×10^{21}	2.24×10^{21}	0.011
	1.7	1.0×10^{-4}	2.09×10^{22}	4.08×10^{21}	0.55
		4.0×10^{-4}	1.56×10^{22}	3.49×10^{21}	0.35
		1.0×10^{-3}	1.07×10^{22}	2.92×10^{21}	0.17
	16.4	4.0×10^{-4}	1.14×10^{22}	3.18×10^{21}	1.23
600	0.16	1.0×10^{-4}	6.76×10^{20}	1.92×10^{21}	0.015
		4.0×10^{-4}	6.08×10^{20}	1.62×10^{21}	0.018
		1.0×10^{-3}	7.21×10^{20}	1.23×10^{21}	0.0095
	1.5	1.0×10^{-4}	5.01×10^{20}	2.42×10^{21}	0.20
		4.0×10^{-4}	8.53×10^{20}	2.09×10^{21}	0.072
		1.0×10^{-3}	7.49×10^{20}	1.97×10^{21}	0.061
	17.0	4.0×10^{-4}	8.98×10^{20}	1.93×10^{21}	1.27

[a] Dose rates and dose levels are defined at the depth at which microscopy was performed.

3. Results

In general, the radiation-induced microstructures were dense, especially at the lower temperatures, but rather simple, being comprised primarily of Frank interstitial loops, some unfaulted perfect loops, some network dislocations, and faceted voids. The density and diameter of the voids and loops observed in the experiments are summarized in Table 1.

As shown in Fig. 2 the swelling of Fe–15Cr–16Ni increases as the dpa rate is lowered at all three irradiation temperatures studied. While swelling appears to increase with increasing temperature, it is significant to note that swelling occurs at 300 °C, a temperature normally thought to preclude swelling in austenitic stainless steels.

Fig. 3 shows that the void density increased somewhat as the dpa rate decreases, although the void density also increases as the irradiation temperature falls. At a given dose level the Frank loop density also increased with decreasing temperature and decreasing dpa rate, as shown in Fig. 4.

4. Discussion

The most significant observation from this study is that swelling can occur at temperatures as low as

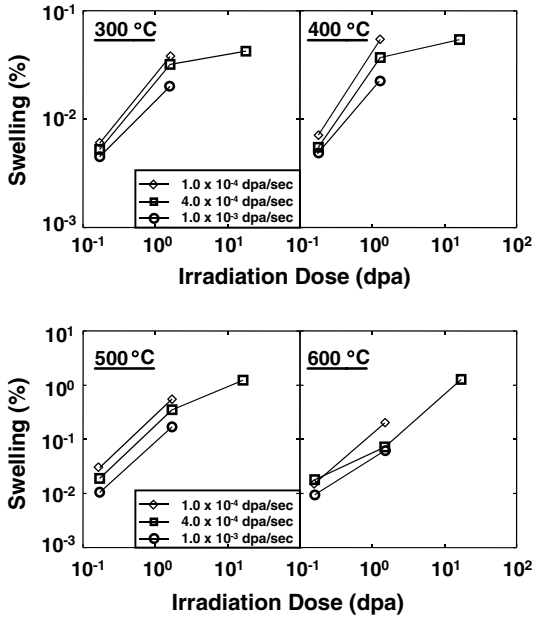

Fig. 2. Dependence of ion-induced swelling of annealed Fe–15Cr–16Ni on temperature, dpa and dpa rate.

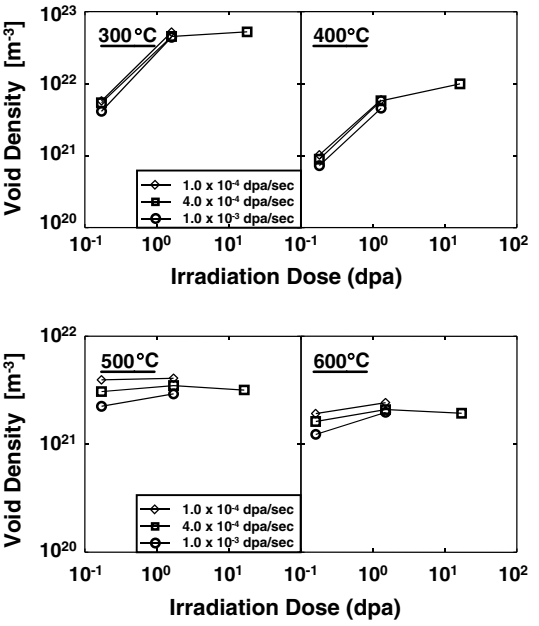

Fig. 3. Dependence of void density of annealed Fe–15Cr–16Ni on temperature, dpa and dpa rate.

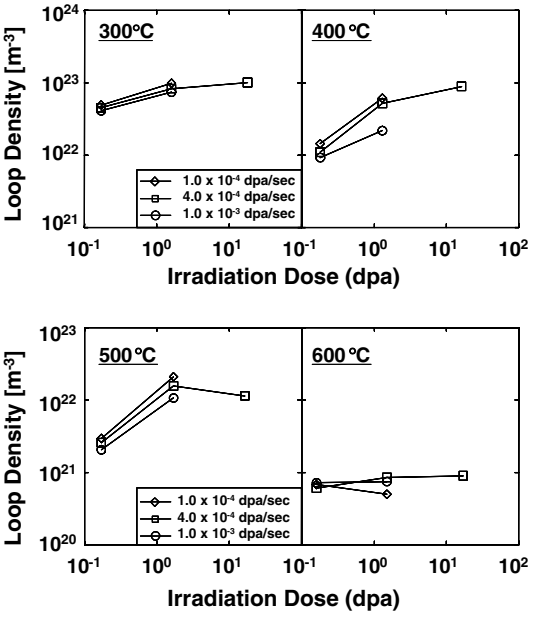

Fig. 4. Dependence of loop density of annealed Fe–15Cr–16Ni on temperature, dpa and dpa rate.

300 °C, even in the absence of injected gases. This result agrees with the results of recent studies on various commercial stainless steels [6–11]. The second important observation is that void swelling was accelerated at lower dpa rates at every temperature studied, and in a manner similar to that of the

companion irradiation study using fast neutrons at ~430 °C [1,2].

When comparing the results of the ion and neutron studies at ~400 °C, it is apparent that the level of swelling obtained at a given dpa level at the very high ion-induced dpa rates is less than that obtained at lower neutron-induced dpa rates, suggesting that dpa rate effects operate regardless of bombarding particle. It must also be recognized, however, that ion-induced swelling tends to be additionally retarded by the combined influence of the surface and the injected interstitial, even when steps are taken to minimize these influences.

The swelling levels attained in this ion experiment have not yet reached sufficiently high levels where it can be determined if changes in dpa rate are expressed primarily in the duration of the transient regime of swelling, as clearly observed in the neutron experiment. However, the ion experiments allow us the opportunity to test the conclusion of the neutron study concerning the origin of the transient shift. In the neutron study, it appeared that the primary dpa rate sensitivity was expressed in the evolution of the Frank loop population and its subsequent unfaulting. At all the neutron-induced dpa rates studied, however, most of the loops had already unfaulted and network formation was well in progress at even the lowest doses studied. In the ion experiment, however, the specimens at the lowest doses still retained most of the Frank loops and a glissile dislocation microstructure was not available to terminate the transient regime.

The loop population at the two lower ion doses decreased with increasing temperature. As shown in Fig. 5, at 16.2 dpa and 400 °C the loop density at 4.0×10^{-4} dpa/s has almost reached saturation at a level consistent with $(\text{dpa rate})^{0.5}$ extrapolation of the ~430 °C neutron data and the models of Watanabe et al. [12] and Muroga and co-workers [13]. At 1.0×10^{-4} dpa/s saturation consistent with this model was reached by ~1 dpa, however, indicating that the saturation dose increases with increasing dpa rate. As the saturated loop density increases with increasing dpa rate, the size of the loops decreases.

When the results of the two companion studies are combined, it appears that the earliest and most sensitive components of microstructure to both temperature and, especially, dpa rate are the Frank loops, whose rate of unfaulting appears to be dependent on size and determines when the glissile dislocation network starts to evolve. The second most sensitive component was found to be the void

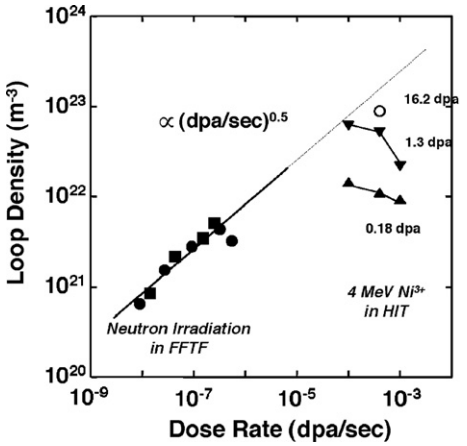

Fig. 5. Dependence of loop density on dpa rate to the 1/2 power, as observed at 400 °C in this experiment and in the companion FFTF experiment. Note that the ion-induced loop density moves toward the trend line of the neutron data with increasing dpa, indicating that saturation of ion-induced loops requires relatively large dpa levels. The dose at which saturation occurs, however, increases with increasing dpa rate.

microstructure, which co-evolves with the loop and dislocation microstructure. It should be noted, however, that loop-dominated microstructures can still allow void formation, but that the growth rate of these voids is restrained until a glissile dislocation microstructure develops.

Based primarily on various neutron and some earlier ion experiments, the dpa rate dependence is manifested primarily in the duration of the transient regime of swelling and not in the steady-state swelling rate.

There are several consequences to these findings. First, most high exposure data are generated in high-flux reactors such as FFTF, guaranteeing that swelling predictions based on these data will significantly under-predict swelling in lower-flux devices or lower-flux positions. Second, the use of ion bombardment studies conducted at greater than reactor-typical dpa rates will further under-predict swelling under reactor-relevant conditions.

5. Conclusions

Over the range of 300–600 °C, the ion-induced void swelling of model Fe–15Cr–16Ni increases as the dpa rate decreases, in agreement with the results of a companion neutron irradiation study on this alloy at ~430 °C. This observation is consistent with a growing body of evidence that void swelling of commercial austenitic alloys increases strongly at

lower dpa rates, primarily by earlier unfaulting of larger Frank loops produced at lower density.

Acknowledgements

This work was supported by Monbusho, the Japanese Ministry of Education, Science and Culture under the FFTF–MOTA collaboration and the JUPITER program (Japan–USA Program for Irradiation Testing for Fusion Research), and the US department of Energy, Office of Fusion Energy under Contract DE-AC06-76RLO 1830 at Pacific Northwest National Laboratory.

References

[1] T. Okita, N. Sekimura, F.A. Garner, L.R. Greenwood, W.G. Wolfer, Y. Isobe, in: Proceedings of the 10th International Conference on Environmental Degradation of Materials in Nuclear Power Systems – Water Reactors, 2001, NACE International, issued on CD format.
[2] T. Okita, N. Sekimura, T. Sato, F.A. Garner, L.R. Greenwood, J. Nucl. Mater. 307–311 (2002) 322.
[3] J.P. Biersack, L.G. Haggmark, Nucl. Instrum. and Meth. 174 (1980) 257.
[4] F.A. Garner, J. Nucl. Mater. 117 (1983) 177.
[5] E.H. Lee, L.K. Mansur, M.H. Yoo, J. Nucl. Mater. 85&86 (1979) 577.
[6] V.S. Neustroev, V.K. Shamardin, Z.E. Ostrovsky, A.M. Pecherin, F.A. Garner, in: International Symposium on Contribution of Materials Investigation to the Resolution of Problems Encountered in Pressurized Water Reactors, September 14–18, 1998, Fontevraud, France, French Nuclear Energy Society, p. 261.
[7] V.S. Neustroev, Z.E. Ostrovskiy, V.K. Shamardin, in: Proceedings of the 7th Russian Conference on Reactor Material Science, September 8–12, 2003, Ministry of the Russian Federation for Atomic Energy, p. 152 (in Russian).
[8] O.P. Maksimkin, K.V. Tsai, L.G. Turubarova, T. Doronina, F.A. Garner, J. Nucl. Mater. 329–333 (2004) 625.
[9] O.P. Maksimkin, K.V. Tsai, L.G. Turubarova, T. Doronina, F.A. Garner, J. Nucl. Mater., these Proceedings.
[10] S.I. Porollo, Yu.V. Konobeev, A.M. Dvoriashin, A.N. Vorobjev, V.M. Krigan, F.A. Garner, J. Nucl. Mater. 307–311 (2002) 339.
[11] F.A. Garner, M.B. Toloczko, J. Nucl. Mater. 251 (1997) 252.
[12] H. Watanabe, A. Aoki, H. Murakami, T. Muroga, N. Yoshida, J. Nucl. Mater. 155–157 (1988) 815.
[13] T. Muroga, H. Watanabe, N. Yoshida, J. Nucl. Mater. 174 (1990) 282.